Title

Predicting the evolutionary dynamics of seasonal adaptation to novel climates in Arabidopsis thaliana

Journal

Proceedings of the National Academy of Sciences of the United States of America, 113(20)

ISSN

0027-8424

Authors

Fournier-Level, Alexandre
Perry, Emily O
Wang, Jonathan A
et al.

Publication Date

2016-05-17

DOI

10.1073/pnas.1517456113

Peer reviewed

Predicting the evolutionary dynamics of seasonal adaptation to novel climates in *Arabidopsis thaliana*

Alexandre Fournier-Level[a,b,1], Emily O. Perry[b], Jonathan A. Wang[b,c], Peter T. Braun[b,d], Andrew Migneault[b,e], Martha D. Cooper[b], C. Jessica E. Metcalf[f,g], and Johanna Schmitt[b,h,1]

[a]School of BioSciences, The University of Melbourne, Parkville, VIC 3010, Australia; [b]Department of Evolution and Evolutionary Biology, Brown University, Providence, RI 03912; [c]Department of Earth and Environment, Boston University, Boston, MA 02215; [d]Department of Biology, California State University, San Bernardino, CA 92407; [e]Everglades Research & Education Center, University of Florida Institute of Food and Agricultural Sciences, Belle Glade, FL 33430; [f]Department of Zoology, University of Oxford, Oxford OX1 3PS, United Kingdom; [g]Department of Ecology and Evolutionary Biology, Princeton University, Princeton, NJ 08544; and [h]Department of Ecology and Evolution, University of California, Davis, CA 95616

Contributed by Johanna Schmitt, February 25, 2016 (sent for review September 3, 2015; reviewed by Jon Ågren, Justin O. Borevitz, and Luis-Miguel Chevin)

Predicting whether and how populations will adapt to rapid climate change is a critical goal for evolutionary biology. To examine the genetic basis of fitness and predict adaptive evolution in novel climates with seasonal variation, we grew a diverse panel of the annual plant *Arabidopsis thaliana* (multiparent advanced generation intercross lines) in controlled conditions simulating four climates: a present-day reference climate, an increased-temperature climate, a winter-warming only climate, and a poleward-migration climate with increased photoperiod amplitude. In each climate, four successive seasonal cohorts experienced dynamic daily temperature and photoperiod variation over a year. We measured 12 traits and developed a genomic prediction model for fitness evolution in each seasonal environment. This model was used to simulate evolutionary trajectories of the base population over 50 y in each climate, as well as 100-y scenarios of gradual climate change following adaptation to a reference climate. Patterns of plastic and evolutionary fitness response varied across seasons and climates. The increased-temperature climate promoted genetic divergence of subpopulations across seasons, whereas in the winter-warming and poleward-migration climates, seasonal genetic differentiation was reduced. In silico "resurrection experiments" showed limited evolutionary rescue compared with the plastic response of fitness to seasonal climate change. The genetic basis of adaptation and, consequently, the dynamics of evolutionary change differed qualitatively among scenarios. Populations with fewer founding genotypes and populations with genetic diversity reduced by prior selection adapted less well to novel conditions, demonstrating that adaptation to rapid climate change requires the maintenance of sufficient standing variation.

climate change | annual plant | genomic prediction | season

Ongoing climate change is causing rapid shifts in environmental selective pressures within local populations (1, 2). To persist, populations must track the shifting multivariate trait optimum by phenotypic plasticity or adaptive evolution (3, 4), or migrate to keep up with poleward shifts in their original climate niche (1). The outcome of these responses to climate change will depend upon the seasonal variation a population experiences, particularly in temperate climates, where seasonality is a major source of environmental heterogeneity (5, 6). Understanding adaptation to seasonal environments is critical for predicting the response to climate change in short-lived organisms with multiple generations per year, like many insects and annual plants. Such prediction requires theoretical projections based on solid empirical foundations, tracking phenotypic change in complex traits as well as in the molecular variation present within populations as they adapt to different seasons. Here, we use a genomic prediction model, based on experimental data from *Arabidopsis thaliana*, to simulate trajectories of adaptation to novel climate scenarios in seasonally variable environments.

In nature, the fitness of an individual is usually determined by multiple correlated traits, each controlled by multiple loci. Natural selection acts simultaneously on all traits and targets multiple loci, creating a whole-genome response to selection. Models of genomic prediction analyze the effect of multiple segregating loci by simultaneously using all genome-wide molecular markers (7). These models assume that traits are additively influenced by every locus of the genome, and attribute a component of the variance to each marker. This modeling approach leads to an explicit decomposition of the genetic architecture of a trait, strictly relying on empirical measures of genetic effects to infer models of evolution. Furthermore, modeling adaptation with realistic genetic effects and genomic positions takes into account the interference between linked loci selected in opposite phase [Hill–Robertson interference (8)], leading to more conservative estimates of evolutionary potential. Such models are of considerable interest for predicting the evolutionary response to climate change in complex environments.

For terrestrial plant populations, the adaptive response to changing climate will involve both plastic and evolutionary responses in fluctuating seasonal environments. Warming temperatures (ignoring the effect of water or nutrient availability) may alter the onset and length of the growing season (9) and also accelerate phenological events, such as flowering (10, 11) and seed maturation (12). However, if temperatures rise beyond plant tolerance thresholds, summer will become unfavorable for growth and survival (13, 14). Also, warmer winters may result in insufficient chilling exposure for floral induction of some species or

Significance

Anticipating the effect of climate change on plants requires understanding its evolutionary consequence on traits and genes in complex realistic environments. How seasonal variation has an impact on the dynamics of adaptation in natural populations remains unclear. We simulated adaptation to different climate change scenarios, grounding our analysis in experimental data and explicitly exploring seasonal variation. Seasonal variation dramatically affected the dynamics of adaptation: Marked seasonality led to genetic differentiation within the population to different seasonal periods, whereas low seasonality led to a single population with fast-evolving fitness. Our results suggest the prevalence of phenotypic plasticity across environmental conditions in determining how climate change will shift selection on traits and loci. In this unpredictable context, maintaining broad genomic diversity is critical.

Author contributions: A.F.-L., J.S., and M.D.C. designed research; A.F.-L., E.O.P., J.A.W., P.T.B., A.M., and M.D.C. performed research; J.A.W. and C.J.E.M. contributed new reagents/analytic tools; A.F.-L. analyzed data; A.F.-L. and J.S. wrote the paper; and C.J.E.M. contributed to writing the paper.

Reviewers: J.Å., Uppsala University; J.O.B., Australian National University; and L.-M.C., CNRS.

The authors declare no conflict of interest.

Data deposition: All scripts have been deposited in the Dryad Digital Repository, https://datadryad.org (DOI: 10.5061/dryad.jn4qq).

[1]To whom correspondence may be addressed. Email: afournier@unimelb.edu.au or jschmitt@ucdavis.edu.

This article contains supporting information online at www.pnas.org/lookup/suppl/doi:10.1073/pnas.1517456113/-/DCSupplemental.

genotypes, delaying or preventing reproduction (15). Thus, adaptation to a warming climate will require an evolutionary response to heterogeneous natural selection across different seasons. Migration poleward to track a population's original temperature conditions also requires adaptation to seasonal changes in day length, with longer days in summer, shorter days in winter, and faster changes in day length in fall and spring (16). Plant reproductive development is often controlled by interacting seasonal cues of photoperiod, ambient temperature, and chilling exposure. Both climate change and poleward migration may create an unprecedented combination of photoperiodic cues and seasonal thermal environments, resulting in novel selective pressures.

Short-lived annual plants capable of multiple generations per year face particular challenges in adapting to novel seasonal environments. Seasonal variation could lead to the maintenance of genetically specialized subpopulations adapted to different seasonal environments (17). Seasonal specialization has two nonexclusive drivers: differences in selection across seasons, resulting in some genotypes being favored over others in a particular season, and nonoverlapping life histories, resulting in a reproductive isolation of subpopulations (18). Seasonally varying selection is a more direct mechanism for adaptive differentiation and does not preclude gene flow across subpopulations, potentially maintaining genetic diversity, whereas life history exclusion would not, per se, increase the adaptive fitness and might eventually erode the genetic basis of the population through drift. However, few studies have investigated the potential for seasonal differentiation. Depending on the specific genetic architecture of traits and fitness in the different seasonal environments, seasonal adaptation may result in selective trade-offs but may also occur through adaptation at season-specific, conditionally neutral loci. Altogether, strong seasonality results in more complex selective environments, with more different and temporary transient optima. Including multiple seasonal cohorts in models of climate adaptation is therefore fundamental to understand the long-term response in temperate environments.

The annual plant *Arabidopsis thaliana* provides an excellent opportunity to model trajectories of adaptation to novel climate scenarios. *A. thaliana* is a widespread species experiencing a wide range of climates. Some populations produce multiple seasonal cohorts per year, including winter annuals as well as rapid cycling cohorts germinating in spring, summer, or early autumn (19). This species shows evidence of adaptation to climate on a broad geographic scale (2, 20–22) as well as along altitude gradients (23–25). Populations are large (26) and geographically structured over multiple spatial scales (27), maintaining extensive genetic variation. Although the species is largely self-fertilizing, outcrossing is not uncommon, allowing recombination to generate new genotypes (28). These properties make *A. thaliana* a powerful model for exploring general features of the evolutionary process leading to adaptation in temporally heterogeneous environments. Finally, the resources available for *Arabidopsis* enable the use of genomic prediction models to dissect the dynamic of this adaptation at the molecular level, genome-wide.

Here, we investigated the short-term dynamic of seasonal adaptation in *A. thaliana* through simulation based on experimental data. In controlled environments, multiple cohorts of a subset of multiparent advanced generation intercross (MAGIC) (29) lines were planted at four different times of the year in four different simulated climates. These climates corresponded to (*i*) a reference (REF) climate set in Norwich (United Kingdom); (*ii*) a climate with a warmer winter (WAW), mimicking the effect of climate change only affecting winter; (*iii*) a climate with a year-round warmer temperature (TEM), corresponding to what plants will face in Norwich in 2100 according to Intergovernmental Panel on Climate Change (IPCC) A1B model predictions (30); and (*iv*) a climate with an increased photoperiod amplitude (PHO), mimicking the seasonal climate poleward migrating plants will have to adapt to. We measured 12 ecologically relevant traits for each plant that defined life history, development, fitness, and offspring germination patterns and recorded mortality. These data were developed into individual-based simulations of adaptive trajectories, by first dissecting the influence of multiple traits on fitness and characterizing the genetic basis of each trait at the SNP level and then tracking over the course of the simulation the change in trait values linked to specific genetic combinations and the change in the overall molecular variation present in the population. The simulation model was designed to reflect an isolated population of fixed size, with recombination from standing variation as the only source of genetic innovation and no de novo mutation. Competition in a fixed-size population then selected particular genotypes based on the empirical measures of traits, depending on the underlying genetic effects. We tested for differences in genetic composition and rate of adaptation across seasons under the different climate scenarios, starting with a broad synthetic base population representing species-wide genetic diversity. We then investigated the effect of adaptation on global genetic diversity as well as for specific loci associated with trait variation. Finally, we tested how easily populations with less genetic variation after being preadapted to a specific environment could readapt to a new environment, mimicking climate change.

Results

Trait Variation Across Climate and Season. For each of the four climates tested, the four cohorts planted through the year (on April 1 for spring, on July 29 for summer, on September 9 for early fall, and on October 14 for late fall) showed extensive plasticity to season of planting and climate treatment (*SI Appendix*, Fig. S1). The effect of climate treatment on trait means differed among seasonal cohorts. All traits exhibited significant genotype-by-season interaction [mixed-linear model (MLM); $P < 10^{-4}$], indicating genetic variation in plasticity to seasonal environment. Days to bolting, weight at harvest, and germination rate of the offspring seeds had the greatest genotype-by-season interaction variance (*SI Appendix*, Fig. S2). By contrast, we observed little genetic variation in plasticity to climate (genotype-by-climate interaction), revealing more potential to evolve in response to seasonal variation than to climate variation alone. This pattern is consistent with the fact that intraannual variation in temperature and photoperiod in this experiment was greater than variation across the climates tested (*SI Appendix*, Fig. S3).

The high correlation among traits revealed strong functional interdependence (*SI Appendix*, Fig. S4). A trait network was used to model trait (co)variation, defining the topology using a backward stepwise method taking germination rate as the most downstream trait, adding each trait iteratively, and allowing a maximum of three upstream connections per trait based on the Bayesian information criterion (BIC). The model that best explained the relationships between traits across all 16 plantings placed days to bolting as the most upstream trait and followed the phenological order of plant life history, with the exception of early growth rate placed downstream of days to bolting, due to its strong correlation with total seed weight (Fig. 1*A*). Total seed weight, seed number, and (seed) dormancy showed the highest connectivity across traits, with three upstream connections each. No trait was left unconnected using the BIC for alternative model comparison. Although the overall topology of the model was fixed across environments based on the experimental data, the variance and covariance between traits based on observed values were allowed to change across seasons and climates, effectively modeling environmental plasticity. Comparison of the predicted values against the observed values for the estimated seed number showed the model fitted the data with good accuracy ($R^2 = 89\%$; *SI Appendix*, Fig. S5). Broad-sense heritabilities ranged from 0 to 0.96 (mean = 0.29 for the 12 traits in 16 plantings), with days to bolting being the most heritable trait, suggesting a strong genetic component. The contribution of individual SNPs to the genetic variance of each trait was calculated using genomic prediction models (*Materials and*

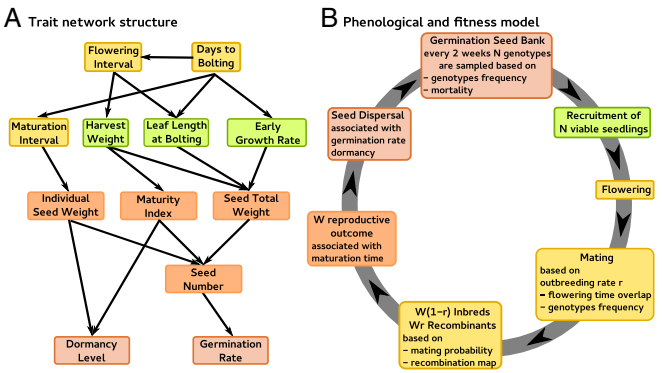

Fig. 1. (*A*) Structure of traits network. This topology was inferred through iterative mixed modeling by jointly using all climates and seasonal plantings. The different colors highlight four different trait functional clusters: life history timing, growth, reproductive fitness, and offspring development. A dynamic view of the network is available at traitnet.adaptive-evolution.org/DynAdapt/TraitNetwork.html. (*B*) Phenological and fitness model. Details are provided in *Materials and Methods*.

Methods) including the fixed effect of upstream traits (Fig. 1*A*). This genomic prediction model was used to simulate over time the adaptation of the experimental population in the four different climates going through yearly seasonal variation (Fig. 1*B*).

Simulation of Population Differentiation, Fitness Change, and Adaptive Trajectory. Starting with the standing genetic diversity present in the 52 MAGIC genotypes, and using a time step of 2 wk between germination cohorts from March 1 until November 15, adaptation was simulated in each of the four climates for 50 y with 250 replicated runs. Populations predominantly remained polymorphic (*SI Appendix*, Table S1), and extinction never occurred. Only in the PHO climate did a single genotype ever reach fixation at appreciable frequency (4.42% of the runs); fixation of a single genotype never happened in more than 1% of runs in the other climates. Even under an equal and continuous germination model limiting the demographic differences between seasons, the genetic differentiation between seasonal cohorts was significant in most runs for the REF and TEM climates [Reynolds, Weir, and Cockerham (RWC) distance; generalized linear model (GLM) testing the within- and between-seasons RWC distance, $P < 0.05$], with distinctive spring, summer, and fall populations (*SI Appendix*, Table S1). Mean genetic distance between seasons was substantially increased in the TEM treatment, suggesting that climate warming may promote genetic differentiation of seasonal subpopulations. In the PHO climate, there was less genetic differentiation among seasonal cohorts than in the REF climate, whereas the WAW climate showed the least differentiation of all climates.

The mean timing of life history events showed some difference across climates, with the most noticeable being accelerated bolting and flowering but longer dormancy of the offspring for the summer cohorts of the TEM climate (*SI Appendix*, Fig. S6). The most diversity in life history strategies was found for the fall cohorts in the PHO climate, where both long- and short-cycling genotypes persisted. The offspring of summer cohorts also germinated over a longer time span than spring or later fall ones, potentially exposing them to a wider range of seasonal climates. Variation in maturation time and levels of dormancy led to broadly overlapping cohorts, leaving the possibility for the reproductive outcome of any cohort to colonize other seasonal niches and interbreed with genotypes from other cohorts. Furthermore, we found no consistent differences across climates in the way the offspring of the

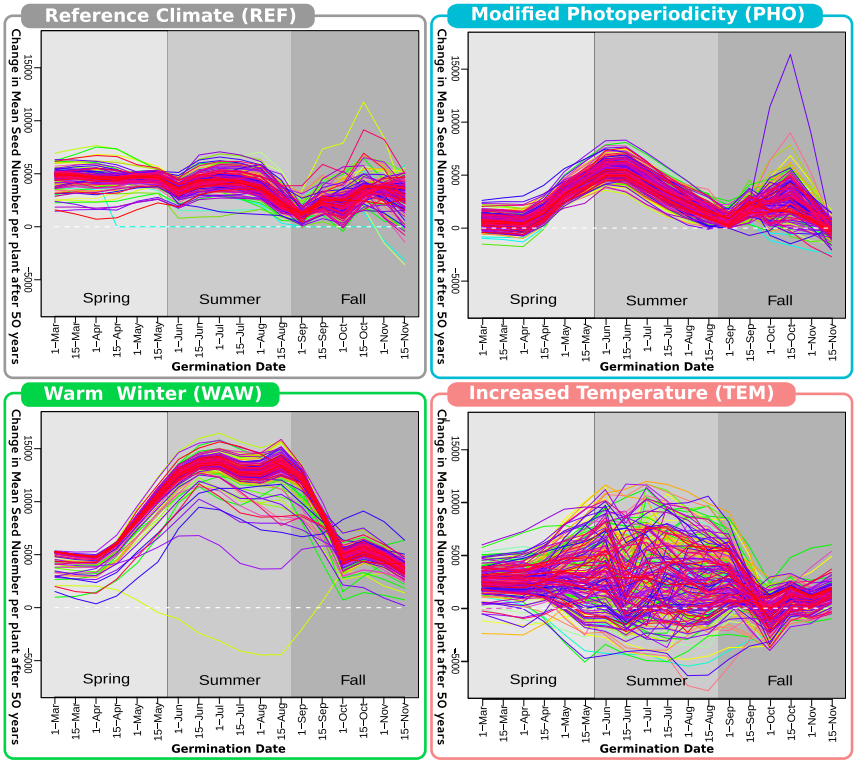

Fig. 2. Change in mean estimated seed number per plant over the year after 50 y of simulation in four experimental climates. The seed number is expressed relative to its mean value in the first year of simulation. Each of the 250 lines corresponds to an independent simulation. The *x* axis represents a set of discrete cohorts germinating at the given dates. Dynamic analysis for all traits can be viewed at traitnet.adaptive-evolution.org/DynAdapt/VideoLauncher.html.

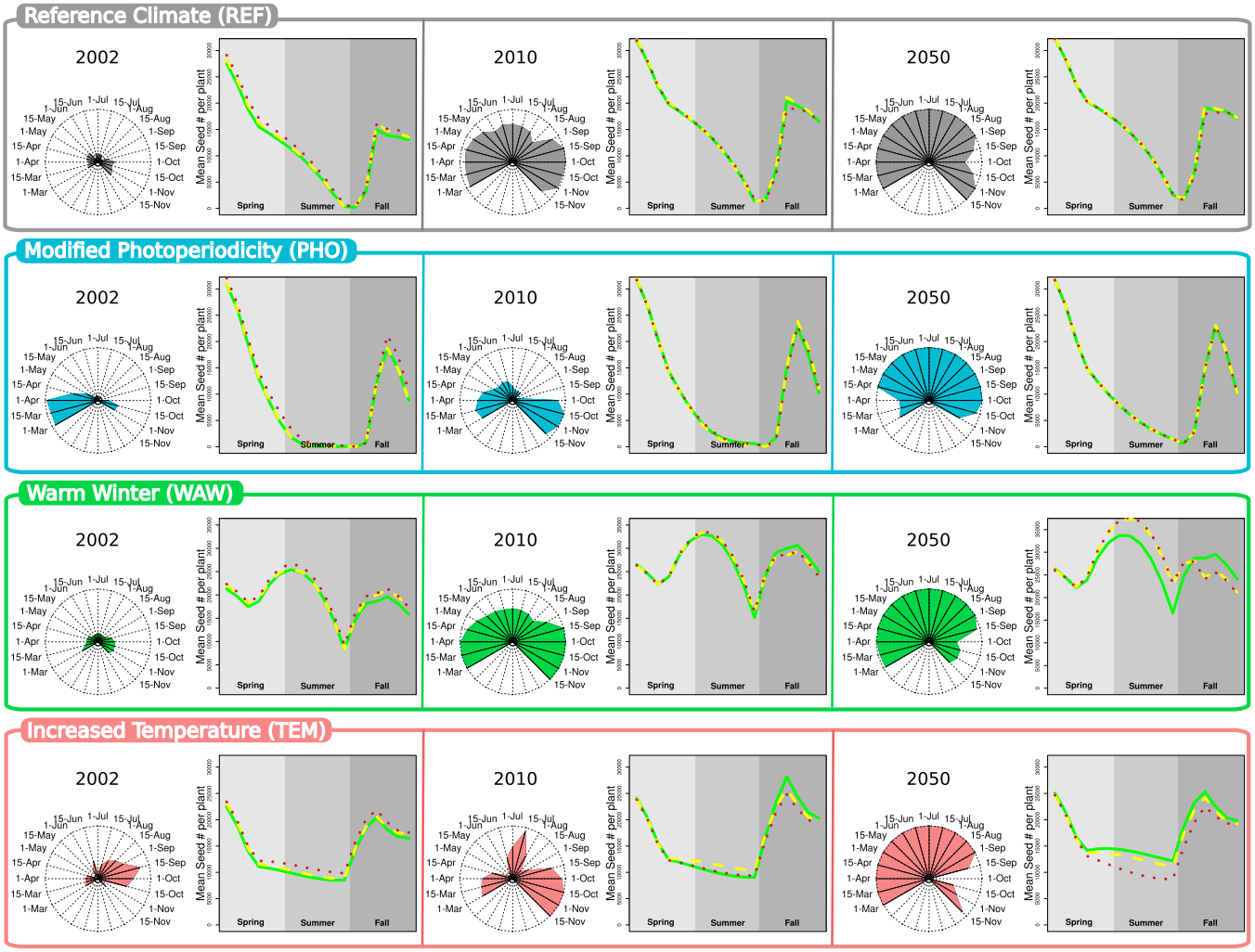

Fig. 3. Seasonal reaction norms of the estimated seed number (*Left*) and mean estimated seed number (*Right*) across replicated simulations over time. For the seasonal reaction norms, each segment of the radar plot represents the normalized mean relative fitness (*y* axis) calculated from 2001 for each germination date (circularized *x* axis), arbitrarily ranging from 0 to 1. A minimum value indicates that the seed number is reaching the minimal seed number for this specific climate at this specific germination date, whereas a maximum value indicates the seed number reaches its maximum over the years. For the mean seed number plot, each curve represents a different cohort transplanted over the year: March 1 spring cohort is shown in solid green, July 1 summer cohort is shown in dashed yellow, and November 15 fall cohort is shown in dotted brown. The *x* axes are identical to the *x* axes in Fig. 2. A dynamic real-time analysis for all traits can be viewed at traitnet.adaptive-evolution.org/DynAdapt/VideoLauncher.html.

different seasonal cohorts overlapped in the seed bank, suggesting no steady pattern of reproductive isolation over time.

The mean estimated seed number per plant, a trait central to fitness in the model, increased for most replicates in all climates, showing the general adaptive potential of the starting population. However, this fecundity increase, a reflection of adaptive success, was uneven across seasons (Fig. 2). The largest increase in fitness was observed for the summer cohorts in the more seasonally equable WAW climate, where the mean seed number per plant increased by more than 25%. Variation between replicates was lower in the PHO climate, and particularly in WAW climate (F test for variance differences, $P < 10^{-5}$). Adaptation was thus rather predictable, with all runs but one yielding similar fitness increases. For the TEM climate, the other climate with a warm winter, the gain in seed number was also potentially greater in summer but differed dramatically across replicates, many of which showed declining fecundity. In this case, successful adaptive evolution depended on newly recombined genotypes (the only source of genetic innovation in the model; *SI Appendix*, Table S1), which were able to take advantage of the summer niche. When analyzing adaptation over time, mean seed number first increased in spring and/or fall and then in summer for all climates (Fig. 3). In the WAW climate, the reduced seasonal differentiation resulted in an initially more even increase across seasons. However, after a phase of general increase, fitness continued to increase in summer but stabilized in spring or decreased in fall, the most striking example of fitness trade-offs across seasons observed in the data. In all climates, we tested in parallel the fitness of the first spring cohort (March 1), the midsummer cohort (July 1), and the last fall cohort (November 15) at every germination date. In general, "home" seasonal cohorts did not outperform "away" cohorts over the longer term when reciprocally transplanted across seasons (Fig. 3). The relative performance of each cohort was transient over the 50 y simulated, with a generally fittest fall cohort early on, progressively matched or outperformed by summer and spring cohorts.

The contribution of each germination cohort to the evolution in the different climates was determined using principal component analysis (PCA) of the matrix of change in mean seed number after 50 y (in each of the 18 two-week cohorts × 250 replicated runs). For all climates except the WAW climate, the first eigenvector, which captured the principal evolutionary dimension, explained between 43% and 49% of the variance in mean seed number per plant. In the WAW climate, the climate with less seasonal differentiation,

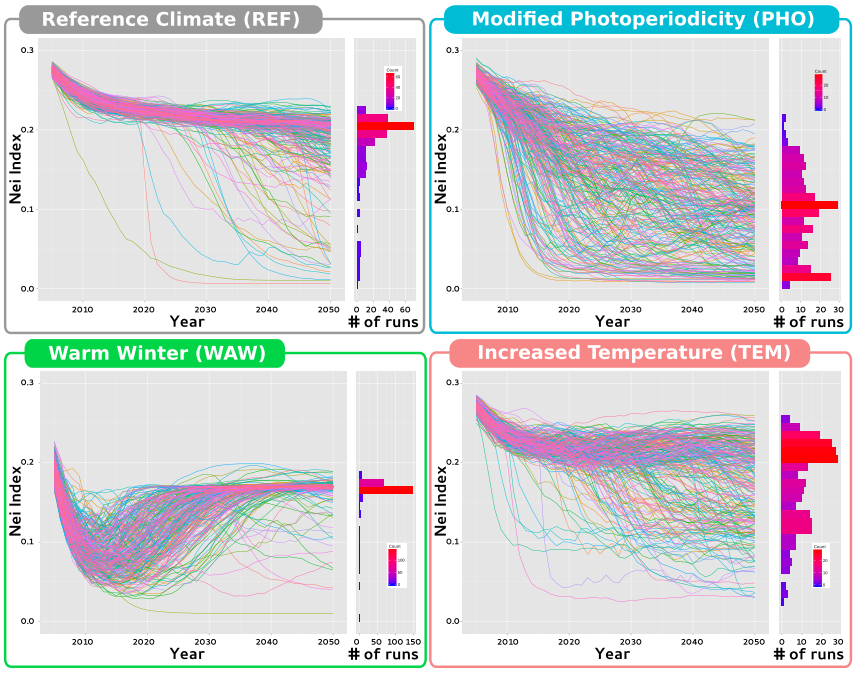

Fig. 4. Evolution of Nei diversity index over 50 y of simulation and histogram of the distribution in 2050. The simulations all started from the same level in 2001, but curves were only plotted from 2005 onward to improve readability.

the first eigenvector explained 64% of the total variance (*SI Appendix*, Table S2), suggesting more variation was accessible along the first evolutionary dimension. We further focused on the three specific cohorts contributing the most to the change in mean seed number; for each climate, these three cohorts corresponded to a spring germination date, a summer germination date, and a fall germination date. Analysis of the first derivatives confirmed adaptation to summer systematically extended for longer periods of time (derivative reaching 0 later; *SI Appendix*, Fig. S7), indicating slower evolutionary dynamics for these cohorts. Also, the fitness increase in summer greatly varied across replicates (Fig. 2), and corresponded to the emergence of recombined genetic variants not initially present in the population (*SI Appendix*, Table S1).

Evolution of the Molecular Diversity and Pattern of Selection for Specific Loci. In all climates, the simulations showed a sharp initial decline in genetic diversity [Nei index (31)], as expected for a population adapting to a novel environment (Fig. 4), with the WAW and PHO climates showing the sharpest decline. After 50 y, the amount of genetic diversity differed across climates, with the REF and WAW climates retaining more diversity and showing reduced variation across replicates (*t* test for mean difference between climates, *F* test for variance difference, $P < 10^{-15}$). In contrast, for the TEM and PHO climates, where overall fitness gain was lower, levels of molecular variation were very variable, with the TEM climate remaining, on average, more diverse than the PHO climate. Interestingly in the WAW climate, with the sharpest initial diversity decrease, the diversity recovered substantially. Increasing the population size led to greater maintenance of diversity in all climates but also to a sharper initial decrease for the WAW and PHO climates (*SI Appendix*, Fig. S8). Increasing the outbreeding rate also increased the mean genetic diversity retained but increased the number of replicates where a few genotypes reached fixation with limited genetic variation remaining. This dual effect illustrates the role of recombination: Between neutral and selected loci, recombination reduces hitchhiking of neutral diversity linked to selected loci (which could otherwise lead to the fixation of a single genotype); between loci selected in the opposite haplotype phase, recombination breaks the linkage between potentially interfering loci, thus increasing selection efficiency (32, 33). Despite consequences at the molecular level, population size and outbreeding rate had a very limited effect on fitness (*SI Appendix*, Fig. S9). The limited effect of demographic parameters indicates that trait evolution is more robust with respect to change in demographic parameters, such as population size and outbreeding, relative to the more sensitive molecular evolution. The model sensitivity to the starting conditions was further tested by initiating the simulation with a set of either two or 10 founder genotypes. As expected, starting with a reduced amount of genetic variation led to the depletion of all genetic diversity (Nei index close to 0) in all climates, with very few instances of a population recovering diversity, even in the WAW climate (*SI Appendix*, Fig. S8). However, the effect of the initial amount of variation at the fitness level was significant in all climates (paired *t* test, $P < 10^{-2}$) except the TEM climate ($P = 0.72$) when comparing 10 and 52 founders (*SI Appendix*, Fig. S9).

To analyze the pattern of selection at specific loci, the probability of fixation for each SNP allele was calculated and compared with its initial frequency (Fig. 5). After removing alleles with an initial frequency greater than 0.95, we considered all alleles whose fixation frequency was greater than the initial allele frequency to be positively selected, under the Wright–Fisher fixation model. In the WAW climate, an important fraction of the alleles reached fixation in a single selection event (25% of the alleles; *SI Appendix*, Fig. S10*C*). A similar pattern was found for the REF (14% of the alleles) climate; however, afterward, a second selection event swept to fixation other alleles with lower initial frequency (*SI Appendix*, Fig. S10*A*). The fixation of this second set of alleles happened after 35 y and corresponded across all runs to the maximum of the derivative for change in seed number, indicating accelerating fitness evolution in fall (GLM, $P < 0.001$; *SI Appendix*, Fig. S7). Allele frequency change thus paralleled fitness trajectories in Figs. 2 and 3, occurring protractedly, first along the first evolutionary dimension for all seasons and then along other dimensions where genetic variance remained, specifically exploiting the fall niche. In the REF and WAW climates, adaptation targeted specific sets of alleles, preserving much of the molecular variation (Fig. 5). Such targeted

sweeps were not observed in the PHO and TEM climates, where, overall, a greater fraction of alleles had a nonnull probability of fixation compared with the REF or WAW climate (*SI Appendix*, Fig. S10 *B* and *D*). In the PHO climate, a greater proportion of rare alleles was targeted, leading to a higher fixation rate overall. When selection targets rare alleles, intense selective sweeps and major loss of diversity can occur; conversely, when selection targets frequent alleles, the loss of genetic diversity caused by hitchhiking of linked loci is limited, even when multiple loci are under selection (34, 35). The sets of selected SNPs did not overlap significantly between climates, except for the SNP selected in the REF climate also showing high fixation probability in the WAW climate (*SI Appendix*, Fig. S11), suggesting a largely independent genetic basis for adaptation across climate. Interestingly, the flowering time gene *FRIGIDA* showed frequent fixation of the *Columbia* deletion allele in the REF climate, which improves fitness in late fall (GLM, $P < 10^{-7}$), whereas the alternative *Landsberg* deletion allele showed more frequent fixation in the PHO climate.

Resilience to Environmental Change. To assess the capacity of the experimental population to transition effectively from the REF climate to the novel ones, the population was preadapted in silico to the REF climate for 10 y, corresponding to the phase with positive derivatives for fitness change in all seasons (*SI Appendix*, Fig. S7) and before fixation of most adaptive alleles (*SI Appendix*, Fig. S10*A*). Climate change was modeled as a gradual change of 1% per year in the regression coefficients over 100 y from the REF climate to the novel climates. Transitioning from the REF climate to the PHO climate is referred to as the Migration scenario, transitioning from the REF climate to the WAW climate is referred to as the Winter Warming scenario, and transitioning from the REF climate to the TEM climate is referred to as the Adaptation scenario. The evolution of seed number differed dramatically between scenarios (*SI Appendix*, Fig. S12). The results showed all possible consequences of climate change on fitness: a strong fitness gain, except for early spring cohorts, for the Winter Warming scenario; a loss of fitness in spring compensated for by a gain in summer and fall for the Adaptation scenario; and a loss of spring and summer fitness and gain in fall fitness for the Migration scenario. Over the course of the climate change simulation, the Nei index went through wave-like fluctuations, whose amplitude depended upon the final climate (REF to PHO > REF to TEM > REF to WAW; *SI Appendix*, Fig. S12).

To distinguish the relative contributions of phenotypic plasticity and genetic adaptation to seasonal fitness changes in each climate change scenario, we performed an in silico "resurrection" experiment, transferring the 2001 initial population to the future climate without evolution. We also reciprocally transferred the 2100 evolved population to the present-day reference climate. The difference in fitness between the 2100 population and the 2001 base population in the future climate thus directly measured the genetic adaptation, whereas the difference between the same population in the two different climates corresponded to the plastic response. Strikingly, the effect of plasticity far exceeded the effect of evolutionary change in all climates (Fig. 6). Fitness was very similar between the 2001 and 2100 populations in either environment, but differed considerably between the current and changed climates for a given population. When the conditions changed toward the PHO or WAW climate, the 2100 population showed some degree of adaptation, outperforming the 2001 population over most of the year until early fall. However, there was no evidence of adaptation in populations transferred to the TEM climate. This lack of adaptive response suggested that initial adaptation to the REF climate fixed a substantial amount of genetic variation, reducing evolutionary potential for subsequent adaptation to the TEM climate. In all three scenarios, when returning both 2001 and 2100 populations back in the present condition, no fitness loss was observed, implying that the 2100 population did not become maladapted to its past climate. With the same framework, we also tested how populations evolved in the steady PHO, WAW, and TEM climates would perform when transplanted to the common REF environment, where they never evolved. Consistent with the previous analysis, no maladaptation was detected, with no difference in mean fitness between the pre- and postadaptation populations and only a slight increase in variance across replicates. This absence of maladaptation reinforces the importance of standing variation in the context of conditional neutrality.

Discussion

Predicting adaptive evolution in a dynamic environment is critical for understanding how populations and species will respond to climate

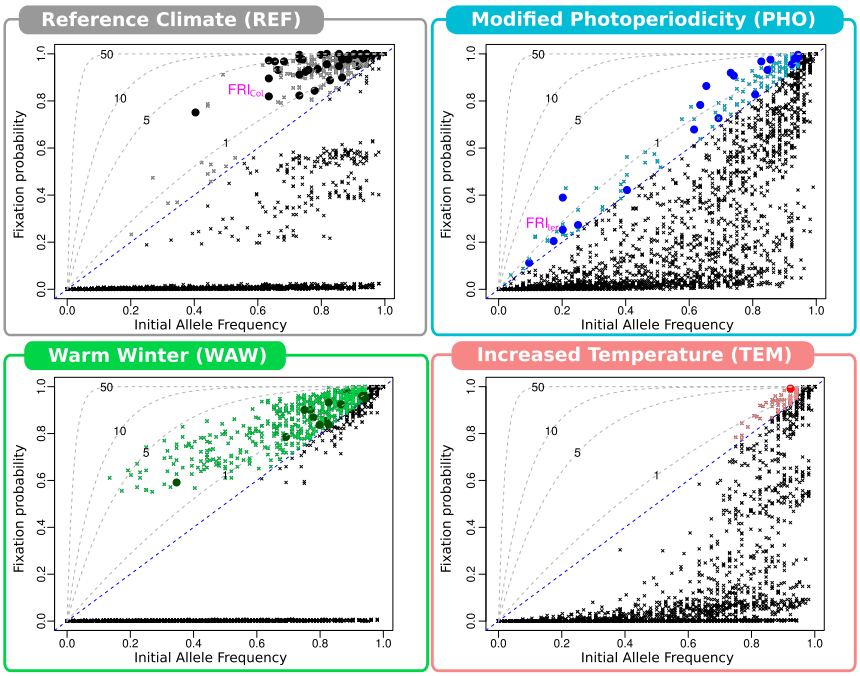

Fig. 5. Probability of fixation for each individual SNP allele in the different climates against the initial allele frequency in the starting population. This probability is calculated as the number of times a given allele reaches fixation across simulation replicates. The dashed line corresponds to the expected values of fixation probability proposed by Fisher and obtained from the diffusion approximation theory for different coefficient of selection in units of $4N_es$. Colored crosses correspond to the alleles considered to have reached fixation more often than expected under neutrality, and were thus considered as selected alleles. Colored dots correspond to those selected alleles that also showed association with a trait through either simple GLMs ($P < 0.001$) or genomic prediction models (SNP effect in top 0.1 percentile). FRI_{Col}, FRIGIDA allele of the Columbia parent; FRI_{ler}, FRIGIDA allele of the Landsberg parent.

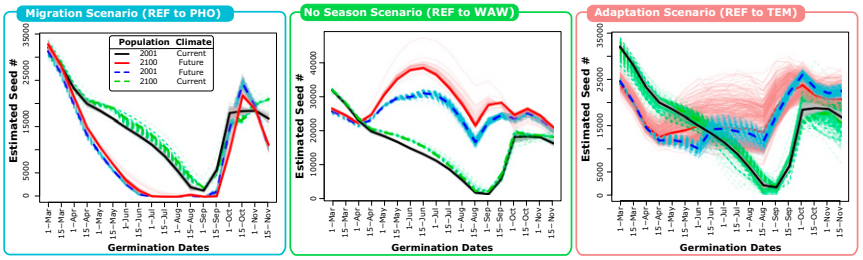

Fig. 6. Absolute mean seed number per plant over the year for 100 y of simulation for three scenarios transitioning from the current REF climate to a novel climate under climate change. Solid lines represent the seed number for the initial population in 2001 under the current climate (black/gray) and for the final population in 2100 after experiencing the future climate (red/pink). Dashed lines represent the reciprocal transplant of the 2001 population directly to the future climate without adaptation (blue/cyan) and of the 2100 population back to the current climate (green/emerald). For each scenario, the thin light lines represent each of the 500 replicated runs and the thick dark lines represent the mean.

change. Empirical studies provide evidence of past adaptation to climate change (36–38), but measuring multigenerational evolutionary response to experimental environmental change is only feasible for organisms with very short life cycles (39, 40, but also refer to 41, 42). Theoretical quantitative genetic models provide important general predictions of phenotypic evolution in response to environmental change (3, 4, 43, 44) but lack biological specificity. Making biologically meaningful predictions is particularly difficult when the traits under selection are plastic and when selective pressures vary temporally over the year. To address this challenge, we used a genomic prediction framework, based on experimental data, to model phenotypes and fitness of different genotypes in complex seasonal environments. We could thus perform in silico experiments exploring the dynamics of phenotypic adaptation and allele frequency change in different climate change scenarios. This approach yielded a number of insights.

Genetic Differentiation Between Seasonal Cohorts. Field studies have revealed multiple seasonal germination cohorts in many *A. thaliana* populations (26, 45, 46), as well as seasonal differences in natural selection on life history traits (47, 48). Moreover, genotypes may differ in phenology and fitness across natural environments (48–51), which may promote reproductive isolation. It is therefore of interest to ask whether genetic differentiation can occur among seasonal cohorts within a population. Our simulation experiments predicted that a genetically variable base population could differentiate genetically into seasonal subpopulations, but the extent of differentiation depended upon climate. Seasonal differentiation between genotypes was enhanced in the TEM climate relative to the REF climate. In contrast, the WAW climate or PHO climate expected with poleward migration considerably reduced this seasonal differentiation. As a consequence, the PHO and WAW climates showed a relatively fast initial decline in genetic diversity (Fig. 4) and the smallest fitness difference between replicates, illustrating how slight changes in climate can profoundly modify the genetic response of plant populations to seasonal variation. Differentiated season-specific populations of annual plants have rarely been reported in the wild (52, 53, but refer to 54), in contrast to algae, insects, or birds (55–57). Our results suggest that seasonal genetic differentiation should be considered in understanding how annual plant populations will respond to climate change.

Without strong evidence of seasonal adaptation at the fitness level or a clear pattern of seasonal reproductive isolation, the mechanism promoting seasonal differentiation remains unclear. An uneven rate of adaptation across seasonal cohorts (*SI Appendix*, Fig. S7), differences in the accessibility of molecular variation (*SI Appendix*, Fig. S10), or differences in the covariance between seasons (*SI Appendix*, Table S2) could provide some degree of explanation. However, when genetic differentiation between seasons was reduced (*SI Appendix*, Table S1), we observed fitness trade-offs as between early summer and fall in the gradual Migration scenario (Movie S1) and as between summer and fall cohorts in the WAW climate (Movie S2). In contrast, when genetic differentiation occurred across seasons (REF and TEM), seasons become the time analog to heterogeneous niches or resources (58), with seasonal cohorts potentially behaving as time-isolated subpopulations and avoiding potential genetic trade-offs. Interbreeding with genotypes migrating from other seasonal cohorts would expose them to a "time-shift meltdown," analogous to the migrational meltdown commonly thought of in the context of spatial variation (59), as in the case of the WAW climate in fall, where mean fitness decreases between 2010 and 2050 (Fig. 3). A consequence is that populations from climates promoting seasonal genetic differentiation are less affected by trade-offs than populations from climates with smoother seasonal contrasts, and may retain more genetic diversity over the adaptation process.

Plasticity of Traits and Genetic Architectures Across Seasons and Climates. Phenotypic plasticity may facilitate evolutionary rescue and adaptation to rapid climate change, allowing novel phenotypes to be expressed and selected in new environments (60, 61). For short-lived organisms, seasonal environmental variation may favor plasticity within populations, and thus contribute to the potential for an evolutionary response to changing climate. Annual plants, such as *A. thaliana*, display substantial plasticity of traits and fitness to seasonal environments, as well as genotype × season interaction (19, 46, 48). Climate variation across seasons is generally greater than variation between alternative climate change scenarios, so we also expect genotype × season interactions to be important for the evolutionary response under climate change (*SI Appendix*, Fig. S2). Plasticity in performance emerged from changes both in the correlation between traits (traitnet.adaptive-evolution.org/DynAdapt/TraitNetwork.html) and in the genetic architecture of individual traits across environments (*SI Appendix*, Fig. S11). The multigenerational simulated resurrection experiments revealed that population mean seasonal fitness could indeed evolve, with adaptation to different seasons creating distinct outcomes for each climate scenario.

When adaptation depended upon disruption of linked genetic variants through recombination, the initial frequency of beneficial alleles in the population critically affected the fate of the overall genetic diversity. The WAW climate showed the fixation of a set of high- to intermediate-frequency alleles, whereas the PHO climate led to the fixation of lower frequency alleles. After the fixation of adaptive alleles, the level of molecular diversity was only restored in the WAW climate following selection for intermediate-frequency alleles (Fig. 4). For low-frequency adaptive alleles in the PHO climate, linked selection led to a dramatic loss of molecular diversity through hitchhiking. Thus, adaptive selection on intermediate-frequency alleles is much more likely to preserve molecular variation in largely self-fertilizing plants compared with de novo mutations starting as unique copies.

The Adaptive Trajectory in Response to Climate Variation. A successful adaptive trajectory is achieved by selecting the appropriate standing

genetic variation to realize the optimal trait combination for each season. Starting from a base population of MAGIC lines that broadly sampled genetic variation across the *A. thaliana* species range, we observed substantial adaptive fitness gain in most of the simulations. Altogether, the model pointed to the relative robustness of fitness adaptation in this base population despite varying population size, outbreeding rate, and the number of founder genotypes. In contrast, molecular variation showed a greater sensitivity to these factors. Such a discrepancy in the rate and intensity of the molecular response to selection compared with phenotypic evolution is widely observed (62). This can be explained by selection acting on fitness and targeting specific loci, whereas the rest of the genome is also submitted to drift, making the neutral molecular variation inherently more sensitive to the stochastic consequence of environmental change. Also, different molecular combinations can result in the same phenotype (63), often leading to a more complex pattern at the molecular level. Phenotypic evolution due to genetic adaptation was generally limited compared with phenotypic plasticity to rapid climate change in the resurrection experiments. If populations are adapted to local climate (e.g., 20), it may be important to enhance evolutionary response to a novel climate by assisting gene flow from other parts of the species range (e.g., 64).

The heterogeneity of the seasonal fitness landscape also led to heterogeneity in the rate of adaptation over the seasons and the years. The race for evolution to keep pace with climate change involves tracking the multiple seasonal fitness optima. Adaptation to multiple optima implies breaking the linkage responsible for genomic interference between beneficial alleles, which depends on the initial frequency of these alleles. In a highly polygenic context, genetic interferences may blur the effect of selection on specific alleles with respect to genomic background variation (65). Our analysis suggests that in a complex environment with high seasonal differentiation, such as the TEM climate, targeting multiple optima with a complex genetic basis is hazardous and suffers a stochastic outcome, as measured by the fitness variation across replicates in Fig. 2.

Seasons are a common source of intraannual environmental variation that may result in complex dynamics of adaptation in annual plant populations. High seasonality could preserve more genetic variation by increasing the dimension of the evolutionary landscape as in the REF and TEM climates. However, the distance between the seasonal optima may become too large to enable consistent evolutionary gain (TEM). In return, low seasonal genetic divergence promotes straightforward adaptation to a specific set of conditions as in the PHO and WAW climates. Nonetheless, in the context of environmental change, if the new conditions, and therefore the new fitness optima, are too far removed from the initial conditions, selection is likely to target low-frequency alleles, which may lead to a dramatic depletion in genetic diversity (PHO).

An important general finding from our experiments is that climate change modifies the genetic basis of fitness. The observations of low overlap between selected loci across climates (*SI Appendix*, Fig. S11) and of no maladaptation to the past climate after adaptation to a novel environment (Fig. 6) both suggest the importance of conditional neutrality, with different loci contributing to adaptation in different climates (20, 66). Consequently, phenotypic adaptation to a given type of climate change is critically sensitive to the availability of appropriate molecular variation, and anticipating which alleles will be adaptive under future climate change will be difficult. Therefore, if phenotypic plasticity across climate interacts with adaptation in an unpredictable fashion, maintaining the maximum of standing variation within populations will be key to preserve the adaptive potential of predominantly selfing temperate annual plants.

Materials and Methods

Design of the Experimental Population. A core collection of 52 genotypes from the MAGIC population (29) was selected to maximize phenotypic diversity for four life history traits (67) and genotypic diversity ensuring the equal representation of the 19 founder genomes based on kinship relationships. The kinship relationships between parents and MAGIC offspring accessions were calculated based on the haplotype-tagging 1,260 SNP markers scattered over the genome and using the "Weighted Alikeness in State" method as implemented in CoCoa software (68). The core collection was designed using the "M-method" as implemented in MSTRAT software (69), giving 12.5% loading to each of the life history traits (days to bolting and leaf length at bolting in both long and short days) (67) and 50% loading to the kinship coefficients.

Climate and Growing Conditions. Climate data based on the Geophysical Fluid Dynamics Laboratory Coupled Model, version 2.X (GFDL CM2.1), under the IPCC Special Report on Emissions Scenarios (SRES) A1B_X1 climate scenario were obtained from the National Oceanic and Atmospheric Administration Geophysical Fluid Dynamics Laboratory (30) (data1.gfdl.noaa.gov/CM2.X/). Minimum and maximum daily temperatures for 2001 and 2099 were extracted from the grid file for a 2.5 × 2.5-km cell located on land over Norwich. Minimum and maximum daily temperatures were interpolated to hourly measures and translated from air to surface temperatures as described by Wilczek et al. (19). Finally, the mean weekly climate was obtained by averaging the daily hourly temperatures and dusk/dawn time over 1 wk, and climate conditions in the growth chambers were updated on a weekly base. The REF conditions were based on the model data for Norwich for 2001; the PHO conditions were recomputed using the same model, with Norwich minimal and maximal temperatures for 2001 and the time of dusk and dawn of a location 12° northward, corresponding to central Scandinavia; the WAW conditions were identical to the REF conditions from simulated February 1 until November 7; and the TEM conditions were based on the IPCC A1B model data for Norwich for 2099. For the REF and PHO conditions, winter was simulated by transferring plants to constant 4 °C chambers from subjective November 7 until February 1, maintaining the Norwich and Scandinavia day lengths, respectively. For the WAW and TEM conditions involving no cold winter, the temperatures of the week of November 30 were looped until February 1 and only the day length changed, keeping the daily mean temperature above 6 °C. Weekly light and temperature profiles for all conditions are presented in *SI Appendix*, Fig. S3. Seeds from The Nottingham Arabidopsis Stock Centre were bulked together under 16 h of light to homogenize maternal effect. For each seasonal planting, seeds were cold-stratified at 4 °C in the dark in water and 0.5% agarose media for 4 d. Five seeds were planted in a 4:1 mix of Promix BX and perlite and kept under constant moisture for 1 wk in a walk-in growth chamber at 22 °C day and 20 °C night temperatures under 14 h of daylight. Individual pots were 5 × 5 × 7.5 cm, set in racks of 2 × 5 and randomized twice a week. After 1 wk, seedlings were thinned to one per pot and transferred into 12 Conviron E7/2 units, with each climate being replicated three times in an independent growth chamber. Bottom watering was applied once a week until saturation with 9 ppm of Scotts 15:5:15 CalMag Special fertilizer per liter of water every other watering.

Traits Measurement, Network, and Genetic Effects Estimation. Once transferred to the chambers, plants were censused twice a week for bolting and flowering date. For the first 3 wk in the chambers (2–4 wk after planting), plants were photographed using a Panasonic DMC-ZS5 camera on a tripod located 1 m above the pots. Pictures were scaled, color-filtered, and color-thresholded with a custom script using ImageJ software (NIH) to determine early growth rate. A plant was considered bolting when the reproductive meristem could be identified; the longest leaf was measured on this date, and bolting was systematically confirmed in the next census. Reproductive branches were inserted as they grew into thinly perforated plastic sleeves to recover all seeds from each plant. Plants were harvested when most of the rosette leaves were senesced. Harvested plants were kept to dry in paper bags for 1 wk in the actual temperature of the chamber. A semiquantitative maturity index (MI) was calculated as MI = 2S − (G + F), where S is the degree of senescence of the rosette (0, partially senesced; 1, mostly senesced; 2, completely senesced), G is the amount of green tissue on the reproductive organs (0, no green; 1, some green; 2, mostly green), and F is the amount of fresh flowers (0, none; 1, a couple; 2, more). Plants were weighed, and total above-ground biomass was recorded; plants were then crushed, and seeds were manually separated from chaff using a 100-μm sieve to record total seed weight. Total seed weight was determined on a high-precision balance, and two batches of ∼100 seeds were then counted and weighed to calculate individual seed mass and used to estimate total seed number. Seeds were then stored in plastic vials closed with cotton stoppers and replaced in their original growth chamber. Three weeks after harvest, seeds were tested for germination. For each harvested plant, five replicates of 10 seeds were assayed on plug trays with 1.75 × 1.75 × 2.5-cm cells filled with Promix BX, saturated with water, and replaced in their original chamber. Germination was scored twice a week over a month, when a radicle had perforated the seed tegument and the germinant was removed. Germination trays were saturated with water and replaced in their chamber. Germination rate (number of seeds germinating

per day) and dormancy (in days) were inferred using linear regression on square-root–transformed data. For each trait in each planting, the variance components were estimated following a mixed-model procedure implemented in the R/lme4 package, where *Climate* and *Season* were defined as fixed effects and all effects involving *Genotype* (*Geno*) were defined as random:

$$Y_{ij} = \mu + Climate + Season + Geno_i + Climate^{*}\, Geno_i + Season^{*}\, Geno_i + \varepsilon_{ij}.$$

Broad-sense heritabilities were calculated in a simplified model, $Y_{ij} = \mu + Geno_i + \varepsilon_{ij}$, as $H^2 = \sigma_{Genotype}/\sigma_Y$. The functional relationships between the 12 experimentally measured traits were identified by a network model fitting optimally the data for all 16 plantings (Fig. 1). This model was built iteratively by first identifying the set of traits that best explained the estimated seed number across all four seasons and four climates in a linear mixed model (based on the Akaike information criterion). The procedure was then repeated iteratively with the newly included set of traits explained by all other traits not already connected to the network until all traits were included. For each genotype i, the model takes the form $Y_{ijk} = \mu + \sum_{p=1}^{n} \beta_{pjk} y_{pjk} + g_i + \varepsilon_{jk}$, where Y is the trait of interest, y_n is a set of $n < 4$ correlated traits, and g is the genetic component of the model. For each genotype, the genetic component g for all 12 traits, as well as the survival rate, was estimated as a breeding value using a genomic prediction method (7) as $g_i = \alpha_i X + \gamma_i A$, where X is the binary SNP matrix and A is the kinship matrix from the information of 1,260 genome-wide SNPs, and the value of the kinship matrix between genotypes was computed using the R/emma package. The solution of the model was obtained using a ridge-regression penalization method as implemented in the R/Bayesian Linear Regression (BLR) package (70). The BLR models were implemented with 11,000 iterations, a burn-in period of 1,000 iterations, and a thinning interval of 100. The parameters of the model are thus a matrix of the regression coefficients, from upstream to downstream traits, and a vector of genotype effects (or breeding values) for each trait, combining the effect of all individual SNP and pedigree relationships estimated through the genomic prediction method. The parameters for the four seasonal plantings were extrapolated into a model of continuous temporal variation through the year by assuming that the value of the regression coefficients between two actual planting dates changes linearly over time. The outcome is presented through a graphic user interface (traitnet.adaptive-evolution.org/DynAdapt/TraitNetwork.html). The functional model presented in Fig. 1 predicts the value of each of the 12 traits for a given genotype and a given germination date. This model was used to simulate the evolution of the experimental plant population in the different climate conditions forward in time. Over the course of the simulation, the two sources of variation across runs were the selection or drift due to the finite carrying capacity of the system, expressed as the population size for the cohorts germinating every 2 wk, and the recombination rate within each cohort.

Model of Adaptation to Climate. Plant adaptation to climate was modeled by simulating the evolution of an isolated population with seasonal cohorts continuously germinating every 2 wk from March 1 until November 15. N plants were sampled based on the germination probability G of genotype i conditional on the frequency of the genotype in the seed bank B and on its survival rate SR measured in the experiment: For the kth germinating plant in [1:N], $Pr(G_k = i) = Pr(B_i(t))Pr(SR_i(t))$. For the first year, each of the initial 52 genotypes from the original population was set to germinate with an equal proportion every 2 wk. The values for traits and survival for each date of the year were computed by linearly interpolating the regression coefficients of the linear model presented in the previous section (traits, covariations, and breeding values) between experimental planting dates. Linear interpolation allowed computation of the trait values over the course of adaptation for each genotype and germination time based on trait covariation, SNP markers, and pedigree information, assuming the relationships between traits (regression coefficients) remained constant over the simulated years and traits are not plastic within a season and climate combination (for each genotype, the trait value equals the genotype mean). To model short-term adaptation to novel conditions, the present study focused on standing variation rearranged by recombination, with no mutation or migration. The probability of a specific pair of genotypes to interbreed was computed as the time of overlap of their flowering times scaled to the longest flowering overlap observed in the cohort multiplied by the frequencies of both genotypes:

$$\text{for genotypes } i \text{ and } j,\ p(I_{ij}) = \frac{\Delta FT_{ij} p(G_i) p(G_j)}{max(\Delta FT)},$$

where

$$\Delta FT_{ij} = max\left(t_{maturing}(i); t_{maturing}(j)\right) - min\left(t_{maturing}(i); t_{maturing}(j)\right).$$

For each pair of outbreeding parents belonging to the same cohort, a recombinant genotype was created based on the average number of crossing-over and genome-wide local recombination rates measured in various F1 populations by Salomé et al. (71).

The seeds produced by each genotype in each cohort were modeled as having matured uniformly over time from 20 d after flowering until rosette senescence/harvest and assigned into 2-wk maturation bins over this period. The seeds of each maturation bin were then distributed into germination bins based on each genotype seed dormancy level and germination rate. We first modeled the germination pattern of seeds germinating the same year (without overwintering) from a normal distribution with a mean equal to the seed dormancy and a variance equal to the germination rate. The seeds left from the first year (before winter) were assigned to a germination bin after winter with a germination pattern modeled as a gamma distribution with a rate equal to the secondary dormancy index, calculated as the dormancy plus the difference between the dormancy in the spring planting and dormancy in the early fall planting, and a shape equal to the germination rate. We used a gamma distribution to model the synchronizing effect of winter chilling so that the probability of germinating before the end of winter is null.

Simulations. The model was written in the R programming language with bash scripts to edit the input files and run the computing. Two sets of simulations were run: either in steady conditions or changing the climate over the course of the simulation. For the steady simulations, each climate adaptation scenario was carried for 50 y with 250 independent runs using different seed values. The climate changed across season over 1 y but remained identical across years. Different combinations of 2-wk cohort population size and outbreeding rate were tested: 100 individuals/10% outbreeding, 1,000 individuals/10% outbreeding, 10,000 individuals/10% outbreeding, 1,000 individuals/5% outbreeding, and 1,000 individuals/20% outbreeding. Sensitivity to initial level of genetic variation was also tested by randomly sampling two of 10 founder genotypes for 500 iterations in each climate. For the changing climate simulations, after a 10-y burn-in period in the REF climate, each climate adaptation scenario was carried for 100 y with 500 independent runs using different seed values. The population size was fixed to 1,000 individuals in each two-week cohort and 10% outbreeding. The climate change scenarios were modeled by updating the regression coefficients between traits and the breeding values for the genotypes by 1% per year from the values in the REF climate toward the value in the altered climates.

Data Analysis. The output of the model included the regression coefficient between traits, together with the breeding value of each genotype for each trait and season. These breeding values allowed computation of the value of any trait for any genotype at any moment of the simulation. The change in mean estimated seed number for each cohort (Δz) was calculated as the weighted mean of the trait within the population in the final year minus the mean estimated seed number for the same cohort in 2001 and taken as the main proxy for fitness. The Δz (18 two-week cohorts × number of replicates matrix) was analyzed using the PCA function of the R/FactoMineR package. The loadings for each eigenvector were extracted, together with the contribution of each specific cohort to their construction. This eigenanalysis allowed determination of the cohort representing the overall evolutionary trajectory of the populations under a given scenario. The output of the model also included the genotype identity and frequency for each 2-wk germination cohort and for each year. Keeping track of the genotype identities and frequencies allowed retrieval of allele frequencies for the 1,260 SNPs characterizing each genotype and computation of measures of molecular diversity. For the within-population measure of diversity, the Nei index was calculated, where L is the total number of loci, and p is the frequency of allele k at locus l. For pairwise population comparison, the closely related RWC genetic distance was calculated as $\sqrt{\frac{\sum_l \sum_k (p_{pop1} - p_{pop2})^2}{2\sum_l (1 - \sum_k p_{pop1} p_{pop2})}}$. The significance of the seasonal differentiation between spring, summer, and fall was assessed by computing the RWC distance for all pairs of 2-wk cohorts (excluding May 15, June 1, August 15, and September 1 as intermediate cohorts not unambiguously representative of a specific season) and testing if the RWC distance was greater between seasons than among seasons. All scripts are available on the Dryad Digital Repository (dx.doi.org/10.5061/dryad.jn4qq).

ACKNOWLEDGMENTS. We thank F. Evans, J. Polien, A. Hersey, and R. Wu for technical assistance and F. V. Jackson and B. Leib for managing the greenhouse facilities. We also thank F. Blanquart, P. C. Griffin, M. Nordborg, A. A. Hoffmann, and the three reviewers for very insightful comments. This work was supported by National Science Foundation Grants IOS 0935589, DEB 1020111, and DEB 1447203 (to J.S.) and Human Frontier Science Program Organization Fellowship LT000907/2012-L (to A.F.-L.).

1. Aitken SN, Yeaman S, Holliday JA, Wang T, Curtis-McLane S (2008) Adaptation, migration or extirpation: Climate change outcomes for tree populations. *Evol Appl* 1(1): 95–111.
2. Wilczek AM, Cooper MD, Korves TM, Schmitt J (2014) Lagging adaptation to warming climate in Arabidopsis thaliana. *Proc Natl Acad Sci USA* 111(22):7906–7913.
3. Chevin L-M, Lande R, Mace GM (2010) Adaptation, plasticity, and extinction in a changing environment: Towards a predictive theory. *PLoS Biol* 8(4):e1000357.
4. Kopp M, Matuszewski S (2014) Rapid evolution of quantitative traits: Theoretical perspectives. *Evol Appl* 7(1):169–191.
5. Roff D (1980) Optimizing development time in a seasonal environment: The "ups and downs" of clinal variation. *Oecologia* 45(2):202–208.
6. Shimadzu H, Dornelas M, Henderson PA, Magurran AE (2013) Diversity is maintained by seasonal variation in species abundance. *BMC Biol* 11:98.
7. Meuwissen THE, Hayes BJ, Goddard ME (2001) Prediction of total genetic value using genome-wide dense marker maps. *Genetics* 157(4):1819–1829.
8. Hill WG, Robertson A (1966) The effect of linkage on limits to artificial selection. *Genet Res* 8(3):269–294.
9. Wu Z, Dijkstra P, Koch GW, Peñuelas J, Hungate BA (2011) Responses of terrestrial ecosystems to temperature and precipitation change: A meta-analysis of experimental manipulation. *Glob Change Biol* 17(2):927–942.
10. Li Y, Cheng R, Spokas KA, Palmer AA, Borevitz JO (2014) Genetic variation for life history sensitivity to seasonal warming in Arabidopsis thaliana. *Genetics* 196(2): 569–577.
11. Anderson JT, Inouye DW, McKinney AM, Colautti RI, Mitchell-Olds T (2012) Phenotypic plasticity and adaptive evolution contribute to advancing flowering phenology in response to climate change. *Proc Biol Sci* 279(1743):3843–3852.
12. Post ES, Pedersen C, Wilmers CC, Forchhammer MC (2008) Phenological sequences reveal aggregate life history response to climatic warming. *Ecology* 89(2):363–370.
13. Sherry RA, et al. (2007) Divergence of reproductive phenology under climate warming. *Proc Natl Acad Sci USA* 104(1):198–202.
14. Mora C, et al. (2015) Suitable Days for Plant Growth Disappear under Projected Climate Change: Potential Human and Biotic Vulnerability. *PLoS Biol* 13(6):e1002167.
15. Bradshaw WE, Holzapfel CM (2008) Genetic response to rapid climate change: It's seasonal timing that matters. *Mol Ecol* 17(1):157–166.
16. Andrés F, Coupland G (2012) The genetic basis of flowering responses to seasonal cues. *Nat Rev Genet* 13(9):627–639.
17. Scheiner SM (2013) The genetics of phenotypic plasticity. XII. Temporal and spatial heterogeneity. *Ecol Evol* 3(13):4596–4609.
18. Vavrek MC, McGraw JB, Yang HS (1996) Within-population variation in demography of Taraxacum officinale: Maintenance of genetic diversity. *Ecology* 77(7):2098–2107.
19. Wilczek AM, et al. (2010) Genetic and physiological bases for phenological responses to current and predicted climates. *Philos Trans R Soc Lond B Biol Sci* 365(1555): 3129–3147.
20. Fournier-Level A, et al. (2011) A map of local adaptation in Arabidopsis thaliana. *Science* 334(6052):86–89.
21. Hancock AM, et al. (2011) Adaptation to climate across the Arabidopsis thaliana genome. *Science* 334(6052):83–86.
22. Ågrena J, Oakley CG, McKay JK, Lovell JT, Schemske DW (2013) Genetic mapping of adaptation reveals fitness tradeoffs in Arabidopsis thaliana. *Proc Natl Acad Sci USA* 110(52):21077–21082.
23. Montesinos-Navarro A, Wig J, Pico FX, Tonsor SJ (2011) Arabidopsis thaliana populations show clinal variation in a climatic gradient associated with altitude. *New Phytol* 189(1):282–294.
24. Montesinos-Navarro A, Picó FX, Tonsor SJ (2012) Clinal variation in seed traits influencing life cycle timing in Arabidopsis thaliana. *Evolution* 66(11):3417–3431.
25. Suter L, Rüegg M, Zemp N, Hennig L, Widmer A (2014) Gene regulatory variation mediates flowering responses to vernalization along an altitudinal gradient in Arabidopsis. *Plant Physiol* 166(4):1928–1942.
26. Picó FX (2012) Demographic fate of Arabidopsis thaliana cohorts of autumn- and spring-germinated plants along an altitudinal gradient. *J Ecol* 100(4):1009–1018.
27. Platt A, et al. (2010) The scale of population structure in Arabidopsis thaliana. *PLoS Genet* 6(2):e1000843.
28. Bomblies K, et al. (2010) Local-scale patterns of genetic variability, outcrossing, and spatial structure in natural stands of Arabidopsis thaliana. *PLoS Genet* 6(3):e1000890.
29. Kover PX, et al. (2009) A Multiparent Advanced Generation Inter-Cross to fine-map quantitative traits in Arabidopsis thaliana. *PLoS Genet* 5(7):e1000551.
30. Delworth TL, et al. (2006) GFDL's CM2 global coupled climate models. Part I: Formulation and simulation characteristics. *J Clim* 19(5):643–674.
31. Nei M (1973) Analysis of gene diversity in subdivided populations. *Proc Natl Acad Sci USA* 70(12):3321–3323.
32. Rouzine IM, Coffin JM (2010) Multi-site adaptation in the presence of infrequent recombination. *Theor Popul Biol* 77(3):189–204.
33. Glémin S, Ronfort J (2013) Adaptation and maladaptation in selfing and outcrossing species: New mutations versus standing variation. *Evolution* 67(1):225–240.
34. Przeworski M, Coop G, Wall JD (2005) The signature of positive selection on standing genetic variation. *Evolution* 59(11):2312–2323.
35. Hermisson J, Pennings PS (2005) Soft sweeps: Molecular population genetics of adaptation from standing genetic variation. *Genetics* 169(4):2335–2352.
36. Franks SJ, Weber JJ, Aitken SN (2014) Evolutionary and plastic responses to climate change in terrestrial plant populations. *Evol Appl* 7(1):123–139.
37. Franks SJ, Sim S, Weis AE (2007) Rapid evolution of flowering time by an annual plant in response to a climate fluctuation. *Proc Natl Acad Sci USA* 104(4):1278–1282.
38. Alberto FJ, et al. (2013) Potential for evolutionary responses to climate change - evidence from tree populations. *Glob Change Biol* 19(6):1645–1661.
39. Bennett AF, Lenski RE (2007) An experimental test of evolutionary trade-offs during temperature adaptation. *Proc Natl Acad Sci USA* 104(Suppl 1):8649–8654.
40. Burke MK, et al. (2010) Genome-wide analysis of a long-term evolution experiment with Drosophila. *Nature* 467(7315):587–590.
41. Scarcelli N, Cheverud JM, Schaal BA, Kover PX (2007) Antagonistic pleiotropic effects reduce the potential adaptive value of the FRIGIDA locus. *Proc Natl Acad Sci USA* 104(43):16986–16991.
42. Fakheran S, et al. (2010) Adaptation and extinction in experimentally fragmented landscapes. *Proc Natl Acad Sci USA* 107(44):19120–19125.
43. Duputié A, Massol F, Chuine I, Kirkpatrick M, Ronce O (2012) How do genetic correlations affect species range shifts in a changing environment? *Ecol Lett* 15(3):251–259.
44. Burger R, Lynch M (1995) Evolution and extinction in a changing environment: A quantitative-genetic analysis. *Evolution (N Y)* 49(1):151–163.
45. Donohue K, et al. (2005) Environmental and genetic influences on the germination of Arabidopsis thaliana in the field. *Evolution* 59(4):740–757.
46. Wilczek AM, et al. (2009) Effects of genetic perturbation on seasonal life history plasticity. *Science* 323(5916):930–934.
47. Donohue K (2002) Germination timing influences natural selection on life-history characters in Arabidopsis thaliana. *Ecology* 83(4):1006–1016.
48. Korves TM, et al. (2007) Fitness effects associated with the major flowering time gene FRIGIDA in Arabidopsis thaliana in the field. *Am Nat* 169(5):E141–E157.
49. Burghardt LT, Metcalf CJE, Wilczek AM, Schmitt J, Donohue K (2015) Modeling the influence of genetic and environmental variation on the expression of plant life cycles across landscapes. *Am Nat* 185(2):212–227.
50. Chiang GCK, et al. (2013) Pleiotropy in the wild: The dormancy gene DOG1 exerts cascading control on life cycles. *Evolution* 67(3):883–893.
51. Méndez-Vigo B, Gomaa NH, Alonso-Blanco C, Picó FX (2013) Among- and within-population variation in flowering time of Iberian Arabidopsis thaliana estimated in field and glasshouse conditions. *New Phytol* 197(4):1332–1343.
52. Haldimann P, Steinger T, Müller-Schärer H (2003) Low genetic differentiation among seasonal cohorts in Senecio vulgaris as revealed by amplified fragment length polymorphism analysis. *Mol Ecol* 12(10):2541–2551.
53. Tsukaya H (2005) Molecular variation of Spiranthes sinensis (Orchidaceae) in Japan, with special reference to systematic treatment of seasonally differentiated groups and a dwarf form, f. gracilis, from Yakushima Island. *J Plant Res* 118(1):13–18.
54. Reisch C, Poschlod P (2008) Land use affects flowering time: Seasonal and genetic differentiation in the grassland plant *Scabiosa columbaria*. *Evol Ecol* 23(5):753–764.
55. Quintero I, González-Caro S, Zalamea P-C, Cadena CD (2014) Asynchrony of seasons: Genetic differentiation associated with geographic variation in climatic seasonality and reproductive phenology. *Am Nat* 184(3):352–363.
56. Malacrida AR, Guglielmino CR, Gasperi G, Baruffi L, Milani R (1982) Spatial and temporal differentiation in colonizing populations of Ceratitis capitata. *Heredity (Edinb)* 69:101–111.
57. Gallagher JC (1982) Physiological variation and electrophoretic banding patterns of genetically different seasonal populations of Skeletonema costatum (Bacillariophyceae). *J Phycol* 18(1):148–162.
58. Østman B, Lin R, Adami C (2014) Trade-offs drive resource specialization and the gradual establishment of ecotypes. *BMC Evol Biol* 14(1):113.
59. Blanquart F, Gandon S (2013) Time-shift experiments and patterns of adaptation across time and space. *Ecol Lett* 16(1):31–38.
60. Lande R (2009) Adaptation to an extraordinary environment by evolution of phenotypic plasticity and genetic assimilation. *J Evol Biol* 22(7):1435–1446.
61. Chevin L-M, Gallet R, Gomulkiewicz R, Holt RD, Fellous S (2013) Phenotypic plasticity in evolutionary rescue experiments. *Philos Trans R Soc Lond B Biol Sci* 368(1610): 20120089.
62. Reed DH, Frankham R (2001) How closely correlated are molecular and quantitative measures of genetic variation? A meta-analysis. *Evolution* 55(6):1095–1103.
63. Woods R, Schneider D, Winkworth CL, Riley MA, Lenski RE (2006) Tests of parallel molecular evolution in a long-term experiment with Escherichia coli. *Proc Natl Acad Sci USA* 103(24):9107–9112.
64. Aitken SN, Whitlock MC (2013) Assisted gene flow to facilitate local adaptation to climate change. *Annu Rev Ecol Syst* 44:367–388.
65. Chevin L-M, Hospital F (2008) Selective sweep at a quantitative trait locus in the presence of background genetic variation. *Genetics* 180(3):1645–1660.
66. Anderson JT, Lee C-R, Mitchell-Olds T (2011) Life-history QTLS and natural selection on flowering time in Boechera stricta, a perennial relative of Arabidopsis. *Evolution* 65(3):771–787.
67. Ehrenreich IM, et al. (2009) Candidate gene association mapping of Arabidopsis flowering time. *Genetics* 183(1):325–335.
68. Maenhout S, De Baets B, Haesaert G (2009) CoCoa: A software tool for estimating the coefficient of coancestry from multilocus genotype data. *Bioinformatics* 25(20): 2753–2754.
69. Gouesnard B, et al. (2001) MSTRAT: An algorithm for building germ plasm core collections by maximizing allelic or phenotypic richness. *J Hered* 92(1):93–94.
70. de los Campos G, et al. (2009) Predicting quantitative traits with regression models for dense molecular markers and pedigree. *Genetics* 182(1):375–385.
71. Salomé PA, et al. (2011) Genetic architecture of flowering-time variation in Arabidopsis thaliana. *Genetics* 188(2):421–433.